RSC Advances

ROYAL SOCIETY OF CHEMISTRY

www.rsc.org/advances

RSC Advances RSCPublishing

Communication

Revisit of the Oxidation Peak in the Cathodic Scan of Cyclic Voltammogram of Alcohol Oxidation on Noble Metal Electrodes

Cite this: DOI: 10.1039/x0xx00000x

Received 00th November 2015,
Accepted 00th November 2015

DOI: 10.1039/x0xx00000x

www.rsc.org/

Yangzhi Zhao, Xuemin Li, Joshua M. Schechter, and Yongan Yang*

This work reports straightforward, intuitive, and convincing evidence to elucidate the origin of the oxidation peak in the cathodic scan of cyclic voltammogram of alcohol oxidation on noble metal electrodes. Consequently, three new indicators are also proposed for assessing the electrocatalytic performance of electrodes.

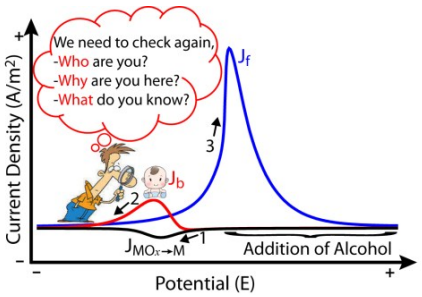

TOC Figure: The origin of the oxidation peak in the cathodic scan of alcohol oxidation is elucidated with suggestion of new performance indicators.

Keywords: Alcohol Oxidation / Fuel Cells / Electrocatalysis / Cyclic Voltammogram / Performance Indicator

1. Introduction

Direct alcohol fuel cells (DAFCs), which "burn" alcohols (such as methanol CH_3OH) at ambient temperatures to generate electricity, are important energy conversion and storage devices for clean and sustainable technologies.[1-5] The electrooxidation of alcohols relies on the catalytic effect of anodes, which are predominantly noble metals and their alloys.[3] In acidic solutions, platinum (Pt) is the most efficient electrocatalyst among all monometallic electrodes.[3] In alkaline solutions, palladium (Pd) turns out to be the most efficient one.[3] Being consistent with the fact that the alcoholic electrooxidation is a multi-electron reaction, a variety of carbonaceous chemicals have been identified as intermediates, among which carbon monoxide (CO) is widely believed to strongly adsorb on the electrode surface and impair the catalytic performance due to the poisoning effect.[6,7] The seriousness of the CO poisoning has long been indexed by an oxidation peak in the cathodic scan of cyclic voltammogram (CV).[6-8] More specifically, the intensity ratio (J_f/J_b) of the peak current in the anodic (forward) scan (J_f) versus that in the cathodic (backward) scan (J_b) is used to describe the "CO-tolerance";[6] the higher the value, the better the tolerance.[9-17] This criterion is generally attributed to a paper published in 1992.[6] The conjecture was based on 1) an assumption that the anodic current beyond the methanol oxidation peak J_f result from oxidation of surface-adsorbed CO to CO_2;[6] and 2) a fact that J_b weakened when the anodic switching potential in the CV was increased.[6,9] Later on, the CO adsorption on electrode surfaces was confirmed by spectroscopic measurements;[7-9] since then, the "J_f/J_b" criterion for indexing the "CO-tolerance" has been widely used in the literature for alcohol fuel cells and referred to for searching high-performance electrocatalysts.[9-21]

In 2012, Tong *et al*. published a pioneering article to question the validity of this criterion for methanol oxidation on Pt/C and PtRu/C electrodes in acidic solutions.[22] By using *in-situ* surface enhanced infrared spectroscopy, they observed that both J_f and J_b presented opposite correlations with the amount of methanol (but not CO) adsorbed on electrode surfaces.[22] The observed correlations underlay the conclusion that both oxidation peaks originated from

the oxidation of surface-adsorbed methanol and the peak intensity ratio was an inadequate parameter to gauge CO-tolerance.[22] However, to date, this opinion has not been well adopted in the community;[23-34] the vast majority of subsequent publications still embrace the old opinion.[10-14,18, 35-84] Some papers quoted both opinions without preference.[85-88] Thus, further clarification on this question is needed.

Herein we provide simple, intuitive, and convincing evidence to clarify the origin of J_b, by revealing the cause-and-effect relationship straightforwardly on the basis of adding alcohol only during the cathodic scan (**Fig. 1**). That is, the apparent J_b is the net current of fresh alcohols' oxidation (J'_b) triggered and counteracted by the reduction of catalyst oxides ($J_{MOx\rightarrow M}$), because 1) the peak potential E_b emerges right after $E_{MOx\rightarrow M}$ and shifts correspondingly when $E_{MOx\rightarrow M}$ changes; 2) J_b is strongly dependent on $J_{MOx\rightarrow M}$, essentially with $J'_b = J_b + J_{MOx\rightarrow M}$; and 3) the occurrence of J_b needs the alcohol to be present *only* before $E_{MOx\rightarrow M}$ during the cathodic scan, where it is impossible to generate CO. Thus, opposite to the conventional criterion, a higher ratio of J_b/J_f is believed to index higher reactivation efficiency, which could actually be more desirable for an electrocatalyst. Additionally, we also propose two other performance indicators to index the activity of a given catalyst, that is, the intensive activity and the extensive activity.

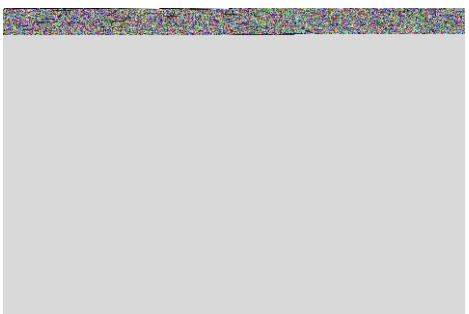

Fig. 1. Typical cyclic voltammograms to study the origin of J_b by adding alcohol during the potential window indicated.

2. Experimental Section

Chemicals: Pd wire (4N, 0.5 mm in diameter), Au wire (4N, 0.5 mm in diameter), and Pt wire (4N, 0.5 mm in diameter) were purchased from ESPI Metals. Sodium hydroxide (NaOH, 99%, Mallinckrodt), methanol (CH_3OH, Pharmco-AAPER, ACS reagent), ethanol (CH_3CH_2OH, Pharmco-AAPER, ACS reagent), were purchased from Fisher. Perchloric acid ($HClO_4$, 70%) was purchased from Sigma-Aldrich. All chemicals were used as received. The nano-pure water (18.2 MΩ cm^{-1}) was from a Barnstead water purification system.

Data Collection: All electrochemical data were collected by using a conventional three-electrode cell controlled by a Reference 600 electrochemical workstation (Gamry Instruments, Inc., USA). The working electrode was a Pd (Au, or Pt) wire with only 5 mm in length exposed in the electrolyte solution; the counter electrode was a coiled Pt wire; and the reference electrode was a saturated calomel electrode (SCE), relying on which the potential versus standard hydrogen electrode (SHE) was calculated. Before being presented in figures, all potentials in the Pd system were further corrected by the IR drop compensation, where R (the solution resistance) was determined via electrochemical impedance spectroscopy (EIS). The EIS was conducted at -0.34 V vs SHE, by applying an alternating voltage of 5 mV in the frequency range of 100 kHz to 10 mHz. As indicated respectively in the manuscript, the electrolyte solution was 0.5 M NaOH, 0.5 M NaOH + 1.0 M CH_3OH, 0.5 M NaOH + 1.0 M CH_3CH_2OH, or 0.1 M $HClO_4$ + 1.0 M CH_3OH. Before the measurement, the electrolyte solution was deaerated by argon for 15-20 mins and maintained with a slight overpressure afterwards. All cyclic voltammograms (CVs) were collected at the potential scan rate of 20 mV/s.

3. Results and Discussion

The Origin of the Referred Oxidation Peak: We initiated our study from observing methanol oxidation on a polycrystalline Pd electrode in alkaline solutions. **Fig. 2A** shows a typical CV of methanol oxidation on Pd in 0.5 M NaOH + 1.0 M CH_3OH, featured with a large J_f and a small J_b. Compared with the CV taken from 0.5 M NaOH without CH_3OH (**Fig. 2B**), two interesting features can be noticed: 1) the anodic current at the potential beyond J_f decreases to virtually zero, which can be assigned to the loss of activity induced by the oxidation of Pd;[33] and 2) the onset (peak) potential of J_b in **Fig. 2A** nicely matches the onset (peak) potential of $J_{PdOx\rightarrow Pd}$ in **Fig. 2B**. From this observation, we hypothesize that the oxidation peak J_b originates from but not merely the oxidation of fresh methanol, and also that the trigger is the reactivation of the previously deactivated electrode surface via reduction of PdO_x.

To prove the hypothesis, we conducted two experiments to monitor their CVs before and after the addition of methanol into the electrolyte solution. In the first case (**Fig. 2C**), one cycle of CV was first collected in 0.5 M NaOH to confirm the normal behavior of Pd as in **Fig. 2B**. Then, after the second anodic scan (line 1), the solution was quickly converted to 0.5 M NaOH + 1.0 M CH_3OH by adding an equal volume of 0.5 M NaOH + 2.0 M CH_3OH into the electrochemical cell. During the potential window of adding methanol (line 2, as indicated), there is *no* generation of CO from the oxidation of methanol within the instrument sensitivity, because the corresponding current is actually zero. Once the potential reached the onset of $J_{PdOx\rightarrow Pd}$ (-0.03 V), an oxidation wave burst and peaked at -0.10 V (line 2), exactly as in **Fig. 2A**. In the subsequent cycles (lines 3 and 4) the J ~ E profiles are virtually identical and both are well consistent with that in **Fig. 2A**. The complete scenario of the CVs before and after the methanol addition is shown in **ESI-Fig. 1**. In the second case (**Fig. 2D**), methanol was not added until the $J_{PdOx\rightarrow Pd}$ peak emerged half way; the cathodic current was immediately reversed into an anodic current.

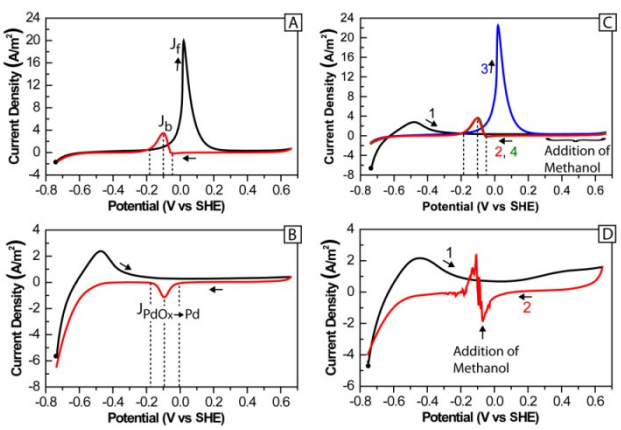

Fig. 2. Study on the origin of the oxidation peak (J_b) in the cathodic scan of CV of methanol oxidation on Pd, by preparing the electrolyte solutions

in different ways. (A) The premade solution of 0.5 M NaOH + 1.0 M CH_3OH; (B) the premade solution of 0.5 M NaOH; (C) the *online* made solution of 0.5 M NaOH + 1.0 M CH_3OH by adding 10.0 mL of 2.0 M CH_3OH/0.5M NaOH into 10.0 mL of 0.5M NaOH solution during the indicated potential window; and (D) the *online* made solution of 0.5 M NaOH + 1.0 M CH_3OH by adding 10.0 mL of 2.0 M CH_3OH/0.5M NaOH into 10.0 mL of 0.5M NaOH solution at the indicated potential.

These results clearly suggest that: 1) $J_{PdOx\rightarrow Pd}$ triggers the occurrence of J_b; 2) the oxidation of CH_3OH but not of CO is responsible for J_b; 3) the pure oxidation current of fresh CH_3OH (J'_b, shown in **ESI-Fig. 2A**) is larger than the apparent current J_b, essentially $J'_b = J_b + J_{PdOx\rightarrow Pd}$; 4) the $J_{PdOx\rightarrow Pd}$ process is not actually suppressed by the J'_b process, but just concealed in the CV; and 5) the oxidized surface is not capable of oxidizing CH_3OH, as supported by the zero anodic current beyond 0.36 V in the anodic scan and between 0.66 V and 0.0 V in the cathodic scan.[33] The last point is also further supported by the fact that there is *no* oxidation current in the anodic scan even if switching the cathodic potential before the occurrence of $J_{PdOx\rightarrow Pd}$ (**ESI-Fig. 3**). Further evidence to support the first four points would be to study the direct electrooxidation of CO. Coincidently, Mota-Lima *et al.* have reported recently that the $J_{PdOx\rightarrow Pd}$ profile during the repeated CV scans showed *no* change when the solution was saturated with CO,[89] which suggested no oxidation of CO in the cathodic scan and its irrelevance to J_b in the presence of CH_3OH. This supports our conclusions above. While some correlation between $J_{MOx\rightarrow M}$ and J_b was proposed by several researchers before,[23,26,33,34] explicit evidence and quantitative analysis of the trigger-consequence relationship were not provided. When studying the oxidation of formic acid in acidic solutions, Conway *et al.* proposed that the observed J_b resulted from an autocatalytic reduction of Pd oxide by formic acid or CO.[90] Thus, the evidence we have presented is convincing and original to prove our hypothesis and elucidate the origin of J_b. Nevertheless, please note that our conclusions here do not conflict with the generation and tolerance of CO during the *forward* scan, as demonstrated many times in the literature.[9-21] Also, we do not mean that there is absolutely no component of CO oxidation in J_b during the *repeated* CV scans in the presence of CH_3OH, but rather we believe that the CO contribution (if any at all) would be below the instrumental detection limit. The CO generated during the forward scan must have been essentially desorbed from the oxidized electrode surface before the potential reaches $E_{PdOx\rightarrow Pd}$. Evidently, a large J_b may not be a bad indication. It would be desirable to establish new criteria associated with J_b for searching high-performance electrocatalysts.

Performance Indicators Associated with the Referred Peak: Next, we would like to understand what more information this peak can disclose for understanding a catalyst's performance. Three interesting questions could be asked: 1) How does this peak (in terms of peak potential and intensity) respond to the oxidation extent of Pd? 2) Is there any correlation between peak J_b (or J'_b) and peak J_f to indicate the catalytic performance of Pd? 3) Can the trigger-consequence relationship be generalized to other alcohols, other catalysts, and acidic solutions?

To answer the first two questions, two series of CV experiments in both the CH_3OH-containing solution and the NaOH-only solution were conducted, by changing the switching potentials in anodic (**Fig. 3**) and cathodic (**ESI-Fig. 4**) scans, respectively. The first glance on **Fig. 3A** (the CH_3OH-containing solution) and **Fig. 3B** (the NaOH-only solution), which study the anodic switching potential (E_+), could come to the following summary: with increasing E_+ (that is, the oxidation extent), E_b and $E_{PdOx\rightarrow Pd}$ both shifted towards more negative, J_b became smaller, $J_{PdOx\rightarrow Pd}$ grew larger; E_f stayed no shift at 0.03 V and J_f grew larger; and the hydrogen adsorption/desorption current due to water-decomposition (below -0.3 V) shrank in the presence of CH_3OH and grew larger in the absence of CH_3OH. As shown in **ESI-Fig. 4**with changing the cathodic switching potential (E_-), none of the three peaks showed appreciable changes; the only change was the expected diminishing of the hydrogen adsorption/desorption current. We note that the dependence of J_b and $J_{PdOx\rightarrow Pd}$ on E_+ is not new in the literature;[6,9,90] however, all explanations are in the context of CO-tolerance but not of J'_b. A further quantitative analysis of the effect of E_+ herein is desired.

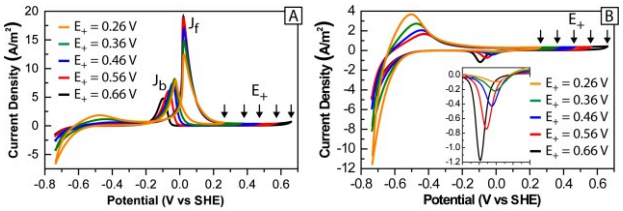

Fig. 3. Study on the effect of oxidation extent of the Pd electrode on J_b and J_f, by tuning the switching potential in anodic scans (E_+ = 0.66 V, 0.56 V, 0.46 V, 0.36 V, and 0.26 V). (A) CVs in 0.5 M NaOH + 1.0 M CH_3OH and (B) CVs in 0.5 M NaOH;

Fig. 4 displays the dependence of various factors on E_+. As shown in **Fig. 4A**, less (or more) positive E_+ induces less (or more) negative $E_{PdOx\rightarrow Pd}$ and E_b as well as larger (or smaller) potential gaps between them. Referring to the literature,[91] the hysteresis for $E_{PdOx\rightarrow Pd}$ can be assigned to the activation energy involved in the place exchange between Pd, OH, and O during both the oxidation and reduction processes. **Fig. 4B** shows that the error of using the apparent peak current J_b instead of the actual methanol oxidation current J'_b could be significant for large E_+. Likewise, the difference between J_b/J_f and J'_b/J_f is also obvious (**Fig. 4C**). The results in **Figs. 4A-4C** show that J'_b would be more appropriate than J_b to index a catalyst's performance and that fair comparisons between different catalysts (particularly across different research groups) require the same experimental conditions, such as the potential window. Since J'_b is induced by and synchronizes with the E_+ dependent $J_{PdOx\rightarrow Pd}$, we term J'_b/J_f as the reactivation efficiency to index how efficient the PdO_x–derived Pd surface is, when compared with the pristine Pd surface. As reported in the literature, J'_b/J_f could be bigger than one.[22,92-94] While the underlying reason is unclear at this moment and also beyond the scope of this work, it might be associated with the formation of advantageous grain boundaries; which have been observed to account for the much superior activity of the oxide-derived copper catalysts to their pristine counterparts in CO reduction.[95,96] Thus, among different catalysts whose other properties are comparable, the one with higher J'_b/J_f might actually be more desirable.

With the elucidation of J'_b to also result from MOR, J'_b needs to be included for indexing the catalytic activity. Different from the conventional style of using only J_f, we

propose using $J_S = J'_b + J_f$ and name it as the intensive activity, since current density is an intensive variable. While current density is used for calculating the power density of a fuel cell, charge density (Q) is required for calculating the energy density. Because J_S could not differentiate catalysts that have comparable peak intensities but different peak widths, we propose a new term – extensive activity ($Q_S = Q'_b + Q_f$), to index a catalyst's activity from a different angle than J_S. As shown in **Fig. 4D**, both J_S and Q_S are strongly dependent on E_+, but in opposite trends. According to J_S, the best E_+ is 0.56 V; according to Q_S, the best E_+ is 0.36 V. This means that both J_S and Q_S are needed to index the activity of a catalyst. The desirable E_+ could then be assigned to a balanced range of [0.36 V, 0.56 V], as indicated by the shadow. In addition, it is noteworthy that the peak potentials in CVs do not describe steady states but dynamic states. Thus, further studies on other properties of the J_f and J'_b peaks are worthwhile.

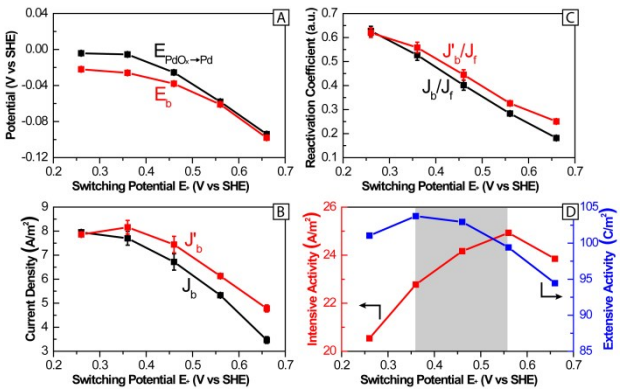

Fig. 4. The dependence of various factors on E_+. (A) E_b and $E_{PdOx\rightarrow Pd}$; (B) J_b and J'_b; (C) J_b/J_f and J'_b/J_f; and (D) $J_S = J'_b + J_f$ (red) and $Q_S = Q'_b + Q_f$ (blue).

Then, we calculated the Tafel slopes (S_T) for J_f and J'_b and employed the technique of differential pulse voltammetry (DPV, **ESI-Scheme 1**).[97,98] **ESI-Fig. 2** shows the J'_b profiles and the corresponding Tafel plots by fitting the linear ranges with $E - E^{o'} = S_T Log(J/J_o)$, where $E^{o'}$ is the formal potential, and J_o is the exchange current density.[97] **ESI-Fig. 5** shows the J_f profiles and the corresponding Tafel plots. The calculated S_T values are graphed against E_+ in **Fig. 5A**. In the range of 0.26 V to 0.36 V, S_T is 115 mV/dec for both J_f and J'_b. With increasing E_+, S_T for J_f increases gradually to 130 mV/dec, consistent with the literature value;[99,100] in contrast, S_T for J'_b decreases to 89 mV/dec. The change of S_T with E_+ reflects the E_+ dependent surface properties.[91,97] $E^{o'}$ for J_f and J'_b are -0.22 V and -0.34V (**ESI-Fig. 6A**), respectively. The corresponding J_o for J_f increases slightly in the range of $10^{-1.54}$ A/m^2 to $10^{-1.20}$ A/m^2 with increasing E_+; and the J_o for J'_b is around $10^{-1.72}$ A/m^2 (**ESI-Fig. 6B**). Different values of $E^{o'}$ and J_o for J'_b and J_f are due to the E_+ dependent oxidation/reduction hysteresis.[91] Now we understand that a larger J'_b associated with a smaller E_+ is essentially due to a larger overpotential $\eta = E_b - E^{o'}$ in addition to a smaller $J_{PdOx\rightarrow Pd}$, despite a larger S_T.[97] **Fig. 5B** shows the plot of current density versus potential measured by DPV, a technique to measure steady states and minimize the capacitive background currents.[97,98] E_f and E_b are observed at 0.03 V and -0.11 V, respectively, which are consistent with those (0.03 V and -0.10 V) in typical CVs. In contrast, the corresponding S_T for J_f has different values in two potential regions (**ESI-Fig. 7A**), that is, 170 mV/dec for [-0.15 V, -0.04 V] and 73 mV/dec for [-0.04 V, -0.01 V]. The corresponding S_T for J'_b is 67 mV/dec (**ESI-Fig. 7B**). The different S_T values indicate different rate determining steps involved in the MOR.[101,102] Overall, this implies that CV seems less sensitive than DPV to determine S_T for multi-electron reactions. Smaller S_T and more negative $E^{o'}$ for J'_b than for J_f indicate that the oxide-derived surface generated during the cathodic scan is more active than the pristine surface in the anodic scan. On the other hand, however, smaller J'_b than J_f could mean that the oxide-derived surface is less stable, as their overpotentials of 0.24 V (η = -0.10 V – (-0.34) V) for J'_b and 0.25 V (η = -0.03 V – (-0.22) V) for J_f are comparable.

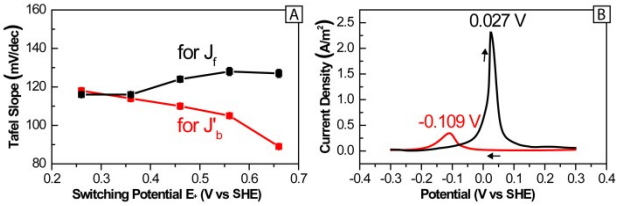

Fig. 5. (A) Tafel slopes for the J_f and J'_b peaks in **Fig. 2A**; and (B) differential pulse voltammogram to determine the relationship of current density versus potential under steady states for Pd in 0.5 M NaOH + 1.0 M CH_3OH.

Generalization of Our Understanding to Other Systems: Furthermore, we would like to test the generality of the trigger-consequence relationship between $J_{MOx\rightarrow M}$ and J_b for other systems. In the case of electrooxidation of ethanol (CH_3CH_2OH) on Pd in an alkaline solution (**Fig. 6A**), we observed the same behavior as for methanol oxidation, except that J_b occurred at a more negative potential (-0.18 V) and J_b/J_f was much larger (0.80), illustrating the high activity of Pd for ethanol oxidation as reported in the literature.[13] Similar phenomenon was also observed for the electrooxidation of CH_3CH_2OH on Au (**ESI-Fig. 8**). In the case of electrooxidation of methanol on Pt in an acidic solution (**Fig. 6B** and **ESI-Fig. 9**),[22] the trigger-consequence relationship between $J_{PtOx\rightarrow Pt}$ and J_b was clearly observed as well. Moreover, as expected, J_b was observed at a more negative potential (0.65 V) than that of $J_{PtOx\rightarrow Pt}$ (0.78 V). The sharp rise of the oxidation current at the methanol addition moment was due to the methanol oxidation on PtO_x surface.[22]

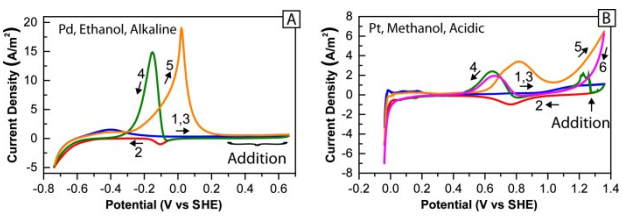

Fig. 6. CVs for electrooxidation of ethanol on Pd electrode in 0.5 M NaOH solution (A) and electrooxidation of methanol on Pt electrode in 0.1 M $HClO_4$ (B). (A) During the first cycle (lines 1 and 2) the solution is 10.0 mL of 0.5 M NaOH. In the second cycle (lines 3 and 4) 10.0 mL of 2.0 M CH_3CH_2OH/0.5 M NaOH is added during the cathodic scan as indicated. Afterwards, another anodic scan (line 5) is conducted. (B) During the first cycle (lines 1 and 2) the solution is 10.0 mL of 0.1 M $HClO_4$. In the second cycle (lines 3 and 4) 10.0 mL of 1.0 M CH_3OH/0.1 M $HClO_4$ is added during the cathodic scan as indicated. Afterwards, another cycle (lines 5 and 6) is conducted.

Last, the scanning electron microscope (SEM) images in **Fig. 7** show the morphologies of the polycrystalline Pd and Pt electrodes used in this work. It is noteworthy that, when using monometallic electrodes, whether the J_b peak occurs or not does not depend on the electrode morphology and feature scale, but its intensity does.[1-4,14-19,22,68,92]

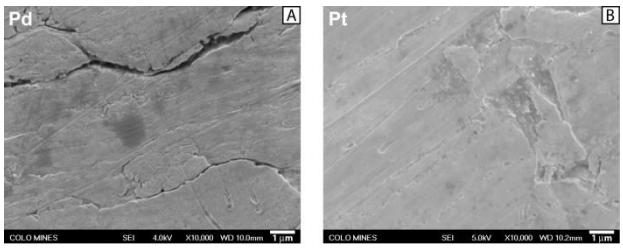

Fig. 7. SEM images of polycrystalline Pd and Pt electrodes used in this study.

3. Conclusions

In summary, we have reported clear-cut and convincing evidence to elucidate the origin of the oxidation peak (J_b) observed in the cathodic scan of cyclic voltammogram of alcohol oxidation on noble metal electrodes. This work corrects a long-held misapprehension of J_b as the oxidation of carbon monoxide and J_f/J_b (J_f is the peak current in the anodic scan) as the indicator of carbon monoxide tolerance, critically amending the previous work by Tong *et al.*[22] In fact, the peak originates from the oxidation of fresh alcohols (J'_b), being triggered and counteracted by the reduction of electrode oxides ($J_{MOx\rightarrow M}$) formed in the proceeding anodic scan. J'_b essentially synchronizes with $J_{MOx\rightarrow M}$. J_b does involve the oxidation of the anodically produced CO. During our preparation of this manuscript, *Tong et al.* further demonstrated that the CO-tolerance is totally irrelevant to the CH_3OH oxidation even in the forward CV scan for a PtRu electrocatalyst.[103] The peak intensity ratio J'_b/J_f, which is strongly dependent on the anodic switching potential (E_+), can indicate the reactivation efficiency of a given electrocatalyst. Two other E_+ dependent performance indicators are also proposed, that is, the intensive activity $J_S = J'_b + J_f$ and the extensive activity $Q_S = Q'_b + Q_f$. Thus, the same experimental conditions, particularly the potential window, are imperative for comparing different catalysts. Smaller Tafel slope (S_T), more negative formal potential ($E^{o''}$) and lower current intensity for J'_b than for J_f indicate that the oxide-derived surface has higher activity but lower stability than the pristine surface. This work suggests new criteria and directions for searching high-performance electrocatalysts used in direct alcohol fuel cells. Intriguing questions for future studies include how the electrode morphology and interface species evolve during the CV scan and how to improve the stability of oxide-derived surfaces.

Acknowledgements

This material is based upon work supported by the Start-up Fund for YY from the Colorado School of Mines.

Notes and references

*Corresponding Author: (Researcher ID: C-2688-2011), Email: yonyang@mines.edu
[a]Department of Chemistry, Colorado School of Mines, Coolbaugh Hall, 1012 14th Street, Golden, CO 80401 U.S.A.

† Electronic Supplementary Information (ESI) available: [More experimental details, cyclic voltammograms, Tafel plots, graphs of formal potentials and exchange currents against the switching potential in anodic scans, and cyclic voltammograms for an Au electrode]. See DOI: 10.1039/b000000x/

References

1 S. Wasmus and A. Kuver, *J. Electroanal. Chem.*, 1999, **461**, 14-31.
2 H. S. Liu, C. J. Song, L. Zhang, J. J. Zhang, H. J. Wang and D. P. Wilkinson, *J. Power Sources*, 2006, **155**, 95-110.
3 C. Bianchini and P. K. Shen, *Chem. Rev.*, 2009, **109**, 4183-4206.
4 X. Zhao, M. Yin, L. Ma, L. Liang, C. P. Liu, J. H. Liao, T. H. Lu and W. Xing, *Energy Environ. Sci.*, 2011, **4**, 2736-2753.
5 Z. Jusys and R. J. Behm, *J. Phys. Chem. B*, 2001, **105**, 10874-10883.
6 R. Manoharan and J. B. Goodenough, *J. Mater. Chem.* , 1992, **2**, 875-887.
7 Y. Zhu, H. Uchida, T. Yajima and M. Watanabe, *Langmuir*, 2001, **17**, 146-154.
8 T. Yajima, H. Uchida and M. Watanabe, *J. Phys. Chem. B*, 2004, **108**, 2654-2659.
9 Z. Liu, X. Y. Ling, X. Su and J. Y. Lee, *J. Phys. Chem. B*, 2004, **108**, 8234-8240.
10 Y. S. Yang, L. Wang, A. Li, Z. J. Jia, Y. Wang and T. Qi, *J. Solid State Electrochem.*, 2015, **19**, 923-927.
11 W. Y. Zhang, H. J. Huang, F. Li, K. M. Deng and X. Wang, *J. Mater. Chem. A*, 2014, **2**, 19084-19094.
12 R. Gupta, S. K. Guin and S. K. Aggarwal, *Electrochim. Acta*, 2014, **116**, 314-320.
13 H. L. Liao, Z. P. Qiu, Q. J. Wan, Z. J. Wang, Y. Liu and N. J. Yang, *ACS Appl. Mater. Interfaces*, 2014, **6**, 18055-18062.
14 Y. Wang, Y. Zhao, W. He, J. Yin and Y. Su, *Thin Solid Films*, 2013, **544**, 88-92.
15 Y. Y. Mu, H. P. Liang, J. S. Hu, L. Jiang and L. J. Wan, *J. Phys. Chem. B*, 2005, **109**, 22212-22216.
16 Z. X. Liang, T. S. Zhao, J. B. Xu and L. D. Zhu, *Electrochim. Acta*, 2009, **54**, 2203-2208.
17 Y. Zhao, L. Zhan, J. Tian, S. Nie and Z. Ning, *Electrochim. Acta*, 2011, **56**, 1967-1972.
18 M. Sawangphruk, A. Krittayavathananon and N. Chinwipas, *J. Mater. Chem. A*, 2013, **1**, 1030-1034.
19 J. Liu, J. Ye, C. Xu, S. P. Jiang and Y. Tong, *Electrochem. Commun.*, 2007, **9**, 2334-2339.
20 J. Sun, J. Shi, J. Xu, X. Chen, Z. Zhang and Z. Peng, 2015, **279**, 334-344.
21 Z. Qi, H. Geng, X. Wang, C. Zhao, H. Ji, C. Zhang, J. Xu and Z. Zhang, 2011, **196**, 5823-5828.
22 A. M. Hofstead-Duffy, D.-J. Chen, S.-G. Sun and Y. J. Tong, *J. Mater. Chem.*, 2012, **22**, 5205-5208.
23 C. S. Sharma, A. S. K. Sinha and R. N. Singh, *Int. J. Hydrog. Energy*, 2014, **39**, 20151-20158.
24 E. N. El Sawy, H. M. Molero and V. I. Birss, *Electrochim. Acta*, 2014, **117**, 202-210.

25 B. J. Plowman, M. E. Abdelhamid, S. J. Ippolito, V. Bansal, S. K. Bhargava and A. P. O'Mullane, *J. Solid State Electrochem.* , 2014, **18**, 3345-3357.
26 P. Hernandez-Fernandez, P. B. Lund, C. Kallesoe, H. F. Clausen and L. H. Christensen, *Int. J. Hydrog. Energy* 2015, **40**, 284-291.
27 M. Rana, M. Chhetri, B. Loukya, P. K. Patil, R. Datta and U. K. Gautam, *ACS Appl. Mater. Interfaces*, 2015, **7**, 4998-5005.
28 Y. Zhao, R. Wang, Z. Han, C. Li, Y. Wang, B. Chi, J. Li and X. Wang, *Electrochim. Acta*, 2015, **151**, 544-551.
29 R. Ojani, J.-B. Raoof and S. Safshekan, *Electrochim. Acta*, 2014, **138**, 468-475.
30 D. Zhang, C. Zhang, Y. Chen, Q. Wang, L. Bian and J. Miao, *Electrochim. Acta*, 2014, **139**, 42-47.
31 X. Xu, Y. Zhou, J. Lu, X. Tian, H. Zhu and J. Liu, *Electrochim. Acta*, 2014, **120**, 439-451.
32 B. Luo, X. Yan, S. Xu and Q. Xue, *Electrochem. Commun.*, 2013, **30**, 71-74.
33 Y. Fan, Z. Yang, P. Huang, X. Zhang and Y.-M. Liu, *Electrochim. Acta*, 2013, **105**, 157-161.
34 X. Xu, Y. Zhou, T. Yuan and Y. Li, *Electrochim. Acta*, 2013, **112**, 587-595.
35 D. Pan, X. Wang, J. Li, L. Wang, Z. Li, Y. Liu, H. Liao, C. Feng, J. Jiao and M. Wu, *Catal. Commun.*, 2015, **62**, 14-18.
36 T. Tomai, Y. Kawaguchi, S. Mitani and I. Honma, *Electrochim. Acta*, 2013, **92**, 421-426.
37 N. Kakati, J. Maiti, S. H. Lee, S. H. Jee, B. Viswanathan and Y. S. Yoon, *Chem. Rev.*, 2015, **114**, 12397-12429.
38 C. Peng, Y. Hu, M. Liu and Y. Zheng, *J. Power Sources*, 2015, **278**, 69-75.
39 A. Renjith and V. Lakshminarayanan, *J. Mater. Chem. A* 2015, **3**, 3019-3028.
40 Q. Dong, Y. Zhao, X. Han, Y. Wang, M. Liu and Y. Li, *Int. J. Hydrog. Energy*, 2014, **39**, 14669-14679.
41 Y.-W. Lee and K.-W. Park, *Catal. Commun.*, 2014, **55**, 24-28.
42 J. Cai, Y. Huang, B. Huang, S. Zheng and Y. Guo, *Int. J. Hydrog. Energy* 2014, **39**, 798-807.
43 L. Dong, X. Tong, Y. Wang, X. Guo, G. Jin and X. Guo, *J. Solid State Electrochem.*, 2014, **18**, 929-934.
44 A. Liu, M. Yuan, M. Zhao, C. Lu, T. Zhao, P. Li and W. Tang, *J. Alloy. Compd.*, 2014, **586**, 99-104.
45 J. R. Rodriguez, R. M. Felix, E. A. Reynoso, Y. Gochi-Ponce, Y. V. Gomez, S. F. Moyado and G. Alonso-Nunez, *J. Energy Chem.*, 2014, **23**, 483-490.
46 L. Wang, Y. Wang, A. Li, Y. Yang, Q. Tang, H. Cao, T. Qi and C. Li, *J. Power Sources*, 2014, **257**, 138-146.
47 L. Wang, Y. Wang, A. Li, Y. Yang, J. Wang, H. Zhao, X. Du and T. Qi, *Int. J. Hydrog. Energy*, 2014, **39**, 14730-14738.
48 Y. Wang, Y. Zhao, J. Yin, M. Liu, Q. Dong and Y. Su, *Int. J. Hydrog. Energy*, 2014, **39**, 1325-1335.
49 H. Yan, C. Tian, L. Sun, B. Wang, L. Wang, J. Yin, A. Wu and H. Fu, *Energy Environ. Sci.*, 2014, **7**, 1939-1949.
50 C. Feng, T. Takeuchi, M. A. Abdelkareem, T. Tsujiguchi and N. Nakagawa, *J. Power Sources*, 2014, **242**, 57-64.
51 V. Kepeniene, L. Tamasauskaite-Tamasiunaite, J. Jablonskiene, J. Vaiciuniene, R. Kondrotas, R. Juskenas and E. Norkus, *J. Electrochem. Soc.*, 2014, **161**, F1354-F1359.
52 E. I. Papaioannou, A. Siokou, C. Comninellis and A. Katsaounis, *Electrocatalysis*, 2014, **4**, 375-381.
53 C.-S. Chen and F.-M. Pan, *J. Power Sources*, 2012, **208**, 9-17.
54 J. Masud, M. T. Alam, Z. Awaludin, M. S. El-Deab, T. Okajima and T. Ohsaka, *J. Power Sources* 2012, **220**, 399-404.
55 Z. Yin, M. Chi, Q. Zhu, D. Ma, J. Sun and X. Bao, *J. Mater. Chem. A* 2013, **1**, 9157-9163.
56 B. Choi, W.-H. Nam, D. Y. Chung, I.-S. Park, S. J. Yoo, J. C. Song and Y.-E. Sung, *Electrochim. Acta*, 2015, **164**, 235-242.
57 M. E. Scofield, C. Koenigsmann, L. Wang, H. Liu and S. S. Wong, *Energy Environ. Sci.*, 2015, **8**, 350-363.
58 L. Zhang, A. Gao, Y. Liu, Y. Wang and J. Ma, *Electrochim. Acta*, 2014, **132**, 416-422.
59 C.-W. Kuo, I. T. Lu, L.-C. Chang, Y.-C. Hsieh, Y.-C. Tseng, P.-W. Wu and J.-F. Lee, *J. Power Sources*, 2013, **240**, 122-130.
60 P. Liu, D. Yang, H. Chen, Y. Gao and H. Li, *Electrochim. Acta*, 2013, **109**, 238-244.
61 Y. Okawa, T. Masuda, H. Uehara, D. Matsumura, K. Tamura, Y. Nishihata and K. Uosaki, *RSC Adv.*, 2013, **3**, 15094-15101.
62 O. Sahin and H. Kivrak, *Int. J. Hydrog. Energy*, 2013, **38**, 901-909.
63 Y.-Y. Yang, J. Ren, H.-X. Zhang, Z.-Y. Zhou, S.-G. Sun and W.-B. Cai, *Langmuir*, 2013, **29**, 1709-1716.
64 S. Ghosh, A.-L. Teillout, D. Floresyona, P. de Oliveira, A. Hagege and H. Remita, *Int. J. Hydrog. Energy* 2015, **40**, 4951-4959.
65 F. Munoz, C. Hua, T. Kwong, L. Tran, T. Q. Nguyen and J. L. Haan, *Appl. Catal. B-Environ.*, 2015, **174**, 323-328.
66 M. I. Prodromidis, E. M. Zahran, A. G. Tzakos and L. G. Bachas, *Int. J. Hydrog. Energy*, 2015, **40**, 6745-6753.
67 C.-L. Sun, J.-S. Tang, N. Brazeau, J.-J. Wu, S. Ntais, C.-W. Yin, H.-L. Chou and E. A. Baranova, *Electrochim. Acta*, 2015, **162**, 282-289.
68 Y. Wang, Q. He, J. Guo, H. Wei, K. Ding, H. Lin, S. Bhana, X. Huang, Z. Luo, T. D. Shen, S. Wei and Z. Guo, *ChemElectroChem*, 2015, **2**, 559-570.
69 P. Mukherjee, P. S. Roy, K. Mandal, D. Bhattacharjee, S. Dasgupta and S. K. Bhattacharya, *Electrochim. Acta*, 2015, **154**, 447-455.
70 W. Chen, Y. Zhang and X. Wei, *Int. J. Hydrog. Energy*, 2015, **40**, 1154-1162.
71 T. Gunji, T. Tanabe, A. J. Jeevagan, S. Usui, T. Tsuda, S. Kaneko, G. Saravanan, H. Abe and F. Matsumoto, *J. Power Sources*, 2015, **273**, 990-998.
72 W. Wang, Y. Yang, Y. Liu, Z. Zhang, W. Dong and Z. Lei, *J. Power Sources*, 2015, **273**, 631-637.
73 P. Wu, Y. Huang, L. Zhou, Y. Wang, Y. Bu and J. Yao, *Electrochim. Acta*, 2015, **152**, 68-74.
74 K. Kakaei and M. Dorraji, *Electrochim. Acta*, 2014, **143**, 207-215.
75 Y.-H. Qin, Y. Li, R.-L. Lv, T.-L. Wang, W.-G. Wang and C.-W. Wang, *Electrochim. Acta*, 2014, **144**, 50-55.
76 Y. Li, L. Yao, L.-Q. Zhang, A.-R. Liu, Y.-J. Zhang and S.-Q. Liu, *J. Electroanal. Chem.*, 2014, **730**, 65-68.
77 A. Sadiki, P. Vo, S. Hu, T. S. Copenhaver, L. Scudiero, S. Ha and J. L. Haan, *Electrochim. Acta*, 2014, **139**, 302-307.
78 Q. Cui, S. Chao, Z. Bai, H. Yan, K. Wang and L. Yang, *Electrochim. Acta*, 2014, **132**, 31-36.
79 W. Hong, J. Wang and E. Wang, *ACS Appl. Mater. Interfaces* 2014, **6**, 9481-9487.
80 J. Friedl and U. Stimming, *Electrochim. Acta*, 2013, **101**, 41-58.

81 R. C. Sekol, M. Carmo, G. Kumar, F. Gittleson, G. Doubek, K. Sun, J. Schroers and A. D. Taylor, *Int. J. Hydrog. Energy*, 2013, **38**, 11248-11255.
82 Z. Yan, J. Xie, P. K. Shen, M. Zhang, Y. Zhang and M. Chen, *Electrochim. Acta*, 2013, **108**, 644-650.
83 S. J. Ye, D. Y. Kim, S. W. Kang, K. W. Choi, S. W. Han and O. O. Park, *Nanoscale*, 2014, **6**, 4182-4187.
84 Z. Yin, Y. Zhang, K. Chen, J. Li, W. Li, P. Tang, H. Zhao, Q. Zhu, X. Bao and D. Ma, *Sci. Rep.*, 2014, **4**, Article No. 4288.
85 S. K. Meher and G. R. Rao, *J. Phys. Chem. C*, 2013, **117**, 4888-4900.
86 R. Wang, D. C. Higgins, M. A. Hoque, D. Lee, F. Hassan and Z. Chen, *Sci. Rep.*, 2013, **3**, Article No. 2431
87 S. K. Meher and G. R. Rao, *ACS Catal.*, 2012, **2**, 2795-2809.
88 Z. J. Mellinger, T. G. Kelly and J. G. Chen, *ACS Catal.*, 2012, **2**, 751-758.
89 A. Mota-Lima, E. R. Gonzalez and M. Eiswirth, *J. Braz. Chem. Soc.*, 2014, **25**, 1208-1217.
90 M. Tian and B. E. Conway, *J. Electroanal. Chem.*, 2005, **581**, 176-189.
91 B. E. Conway, *Prog. Surf. Sci.*, 1995, **49**, 331-452.
92 K. Ding, Y. Zhao, L. Liu, Y. Li, L. Liu, Y. Wang, H. Gu, H. Wei and Z. Guo, *Electrochim. Acta*, 2015, **176**, 1256-1265.
93 Y. Wang, Q. He, K. Ding, H. Wei, J. Guo, Q. Wang, R. O'Connor, X. Huang, Z. Luo, T. D. Shen, S. Wei and Z. Guo, *J. Electrochem. Soc.*, 2015, **162**, F755-F763.
94 K. Ding, Y. Wang, H. Yang, C. Zheng, YanliCao, H. Wei, Y. Wang and Z. Guo, *Electrochim. Acta*, 2013, **100**, 147-156.
95 C. W. Li, J. Ciston and M. W. Kanan, *Nature*, 2014, **508**, 504-507.
96 A. Verdaguer-Casadevall, C. W. Li, T. P. Johansson, S. B. Scott, J. T. McKeown, M. Kumar, I. E. L. Stephens, M. W. Kanan and I. Chorkendorff, *J. Amer. Chem. Soc.*, 2015, **137**, 9808-9811.
97 A. J. Bard and L. R. Faulkner, *Electrochemical Methods: Fundamentals and Applications*, John Wiley and Sons Inc., 2001.
98 A. Molina, E. Laborda, E. I. Rogers, F. Martinez-Ortiz, C. Serna, J. G. Limon-Petersen, N. V. Rees and R. G. Compton, *J. Electroanal. Chem.*, 2009, **634**, 73-81.
99 R. N. Singh and R. Awasthi, *Catal. Sci. Technol.*, 2011, **1**, 778-783.
100 L. V. Kumar, S. A. Ntim, O. Sae-Khow, C. Janardhana, V. Lakshminarayanan and S. Mitra, *Electrochim. Acta*, 2012, **83**, 40-46.
101 E. Herrero, K. Franaszczuk and A. Wieckowski, *J. Phys. Chem.*, 1994, **98**, 5074-5083.
102 M. T. M. Koper, *Fuel Cell Catalysis: A Surface Science Approach*, A John Wiley & Sons, Inc., Hoboken, New Jersey, 2009.
103 D.-J. Chen and Y. J. Tong, *Angew. Chem. Int. Ed.*, 2015, **54**, 9394–9398